Integrative Biology

RSC Publishing

PAPER

View Article Online
View Journal | View Issue

Cite this: *Integr. Biol.*, 2013, **5**, 543

Mathematical modelling of miRNA mediated BCR.ABL protein regulation in chronic myeloid leukaemia *vis-a-vis* therapeutic strategies†

Malkhey Verma,‡§[a] Ehsan Ghayoor Karimiani,‡[bc] Richard J. Byers,[de] Samrina Rehman,[a] Hans V. Westerhoff*[afgh] and Philip J. R. Day*[b]

Received 27th September 2012,
Accepted 4th January 2013

DOI: 10.1039/c3ib20230e

www.rsc.org/ibiology

Chronic myeloid leukaemia (CML) is a clonal myeloproliferative disease resulting from an aberrant BCR.ABL gene and protein. To predict BCR.ABL protein abundance and phosphorylation in individual cells in a population of CML cells, we modelled BCR.ABL protein regulation through associated miRNAs using a systems approach. The model rationalizes the level of BCR.ABL protein heterogeneity in CML cells in correlation with the heterogeneous *BCR.ABL* mRNA levels. We also measured *BCR.ABL* mRNA and BCR.ABLp phosphorylation in individual cells. The experimental data were consistent with the modelling results, thereby partly validating the model. Provided it is tested further, the model may be used to support effective therapeutic strategies including the combined application of a tyrosine kinase inhibitor and miRNAs targeting BCR.ABL. It appears able to predict different effects of the two types of drug on cells with different expression levels and consequently different effects on the generation of resistance.

Insight, innovation, integration

The study has embarked to comprehend the BCR.ABL regulatory pathway and has employed a relatively simplistic model that only takes into account the key components of BCR.ABL onco-protein biosynthesis. We have employed quantitative measurements of BCR.ABL mRNA and phosphorylated protein molecules from single cells, and these data have been integrated and applied to mathematical models of the disease. The 'molecules from single cell' resolution offered by this investigation is intended to help understand the BCR.ABL regulatory pathway, reveal targets and direct therapeutic strategies for treatment of chronic myeloid leukemia.

[a] *Manchester Centre for Integrative Systems Biology, Manchester Institute of Biotechnology, School for Chemical Engineering and Analytical Science, University of Manchester, Manchester, M1 7DN, UK. E-mail: malkhey.verma@manchester.ac.uk, samrina.rehman@manchester.ac.uk*
[b] *Quantitative Molecular Medicine Research, Faculty of Medical and Human Sciences, Manchester Institute of Biotechnology, University of Manchester, Manchester, M1 7DN, UK. E-mail: philip.j.day@manchester.ac.uk*
[c] *Department of New Sciences and Technology, Mashhad University of Medical Sciences, Mashhad, Iran*
[d] *Dept of Histopathology, Manchester Royal Infirmary, Manchester, M13 9WL, UK. E-mail: r.byers@manchester.ac.uk*
[e] *Institute of Cancer Sciences, Faculty of Medical and Human Sciences, The University of Manchester, Manchester, UK*
[f] *Synthetic Systems Biology, Swammerdam Institute for Life Sciences, University of Amsterdam, Amsterdam, Netherlands*
[g] *Department of Molecular Cell Biology, Netherlands Institute for Systems Biology, VU University Amsterdam, Amsterdam, Netherlands. E-mail: h.v.westerhoff@uva.nl*
[h] *Doctoral Training Centre ISBML, The Manchester Centre for Integrative Systems Biology, University of Manchester, Manchester, M1 7DN, UK*

† Electronic supplementary information (ESI) available. See DOI: 10.1039/c3ib20230e

‡ Contributed equally.

§ For queries on clinical aspects of the study contact Ehsan Karimiani, E-mail: ehsan.gh@manchester.ac.uk; Philip Day, E-mail: philip.j.day@manchester.ac.uk. For the modelling component of the study contact Malkhey Verma, E-mail: malkhey.verma@manchester.ac.uk. For systems biology contact Hans Westerhoff E-mail: h.v.westerhoff@uva.nl

Introduction

Chronic myeloid (or myelogenous) leukemia (CML) is a malignant myeloproliferative disorder characterised by the unregulated proliferation of myeloid cells that derive from an abnormal haemopoietic stem cell. CML is considered to be a clonal stem cell disorder subsequent to proliferation of mature granulocytes and their precursors.[1] Specific chromosomal abnormalities are regularly detected in certain human haematological malignancies. For CML this is the 'Philadelphia chromosome', a reciprocal translocation between chromosome 22 and chromosome 9, t(9;22)(q34;q11), which serves CML diagnosis and prognosis.[2]

There is strong evidence that malignant alterations of haematopoietic cells by BCR.ABL protein (BCR.ABLp) rely on its tyrosine kinase (TK) activity. Several signalling pathways are triggered in a kinase-dependent manner and phosphorylated BCR.ABL regulates the expression of various genes implicated in the pathogenesis of CML.[3] The tyrosine kinase activity of BCR.ABL is highly susceptible to tyrosine kinase inhibitors (TKIs) such as imatinib mesylate.[4] BCR.ABL affects the binding and/or phosphorylation of intracellular signalling molecules,

inclusive of FAK (Focal Adhesion Kinase), paxillin, CRKL (Crk-like), CBL (Casitas B-lineage), Grb (Growth factor receptor-bound) and PI3-K (PI3-Kinases).[5] The corresponding signalling pathways may be responsible for abnormal integrin function, which disturbs the regulation of cell proliferation and apoptosis.[6] In addition, BCR.ABL positive cells harbour chimeric kinases that are active constitutively, with their tyrosinesphosphorylated.[7,8]

Cell adhesion appears to play a role in the resistance to apoptosis induced by cytotoxic drugs, including the resistance that is induced by imatinib mesylate treatment.[9] One approach to analysing the association of BCR.ABL with increased adhesion is to investigate expression patterns in single cells. A subpopulation of CML cells with variable malignant properties may then be investigated, in terms of the adherence to plastic, which is characteristic of such leukaemic cells. Currently, there are very few, if any, studies of the association of BCR.ABL expression with adhesion of CML single cells.

Imatinib is a competitive inhibitor of ATP binding to BCR.ABL protein. It thereby inhibits the cell proliferation signal of BCR.ABL and induces cell death in BCR.ABL positive cells.[10] In patients with newly diagnosed CML, TKIs including imatinib are offered as a front-line therapy. While the advent of TKIs has significantly changed the management of the chronic phase of CML, these drugs are not able to entirely eradicate the disease. This could be in part due to rapidly induced or selected cytogenetic changes which occur in the majority of CML patients. imatinib may not, as was long believed, function by its binding to the BCR.ABLp ATP-binding site.[11] With the binding of imatinib, the ABL part of the proto-oncogene may be trapped in a state without kinase activity.[12] Despite some therapeutic success of imatinib, it fails to eradicate leukaemic cells completely.[13,14]

The role of microRNAs (miRNAs) in *BCR.ABL* mRNA expression has been documented.[15] miRNAs are non-coding RNAs 18–25 nucleotides in length that regulate important gene-mediated events by silencing mRNA expression of specific target genes.[16] Some proteins involved in hematopoiesis, such as PRDM5, are capable of transcriptionally regulating other protein-coding miRNAs, which may act as repressor proteins (Rp).[17] Over 1000 miRNAs are encoded by the human genome, including 250 to 600 miRNAs that are conserved across vertebrates.[18]

In recent years evidence has accrued for dysregulation of miRNA expression in cancer cells, resulting in various malignancies,[19] and expression of specific miRNAs correlated markedly with some types of solid cancers.[20] The changes in miRNA expression may modulate specific tumour suppressors or oncogenes that are associated with the development of human cancers.[21,22] Certain miRNAs modulate epigenetic changes, which direct down-regulation of target oncogenes. This suggests possible drug application.[23] Indeed, miRNAs can significantly alter levels of expression in human malignancies.[24] Thus, the changes in expression of miRNAs may play a role in clinical outcome in human cancer.[25]

BCR.ABL protein (BCR.ABLp) is believed to up-regulate oncogenic miRNAs that reduce the expression of tumour suppressor proteins, which should lead to malignant transformation.[15] *BCR.ABL* mRNA has also been shown to be a target of some of the miRNAs such as miR-203: Silencing of miR-203 led to up-regulation of BCR.ABLp in various haematological malignancies, whereas restoration of miR-203 in CML cells resulted in the down-regulation of BCR.ABLp and a reduced proliferation of cancer cells.[26] Therefore, miRNAs may negatively regulate BCR.ABLp expression. Previous studies have also investigated the activity of BCR.ABLp in down-regulation of miR-451[27] and because miR-451 may target and reduce BCR.ABLp suppression,[28] this suggests a reciprocal regulatory loop between miR-451 and BCR.ABLp expression (Fig. 1).

Abnormal expression of miRNAs in CML has been documented by different groups,[19,29–31] and some of these studies reported a significant relationship of miRNAs with BCR.ABL kinase activity.[27,30] Synthetic anti-BCR.ABL small interfering RNA (siRNA) reduced *BCR.ABL* mRNA by up to 87% in cells from CML patients.[32] ABL was shown to be directly targeted by different miRNAs such as miR-203 and miR-130a.

Some crucial questions related to the interplay between BCR.ABLp positive CML, imatinib and miRNAs remain unanswered.

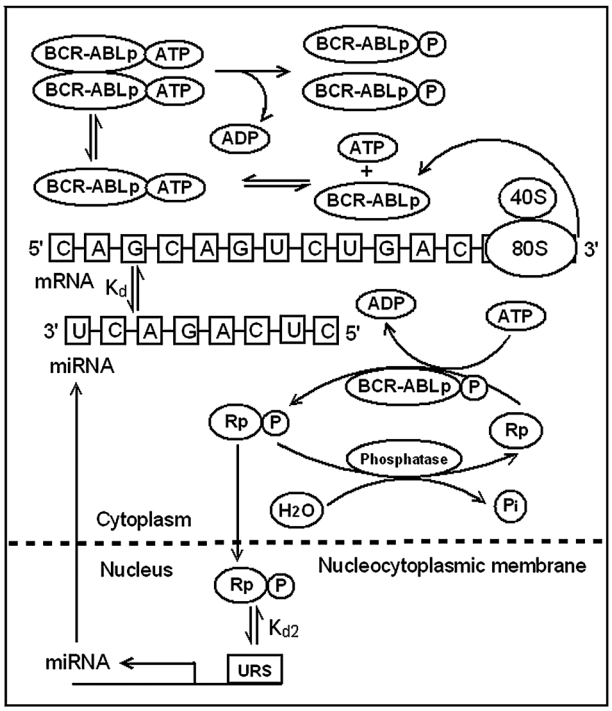

Fig. 1 Relationship between miRNAs and BCR.ABL protein expression incorporating a reciprocal regulatory loop: schematic of miRNA-mediated repression of *BCR.ABL* mRNA translation to BCR.ABL protein (BCR.ABLp) and BCR.ABLp mediated de-repression of its own mRNA translation in CML. BCR.ABLp autophosphorylates upon dimerization of BCR.ABLp–ATP complexes to produce phosphorylated BCR.ABLp (BCR.ABLp ~ P) which is the active form of BCR.ABLp. BCR.ABLp ~ P phosphorylates the transcriptional repressor protein (Rp) responsible for repression of associated miRNA. In the nucleus the phosphorylated form of Rp (Rp ~ P) interacts with upstream repression sequence (URS) of the miRNA gene sequences and represses expression of the latter, consequently de-repressing the *BCR.ABL* mRNA translation. Dissociation equilibrium constants (K_d's) are assumed for interaction of various molecules in the translation and signalling mechanism.

What are the dynamics of imatinib resistance? What effect do TKIs exert on the different sub-populations of leukaemic cells? How can miRNA replacement therapy be effective? The answers to these questions are important for successful treatment of CML patients. A systems biology approach might help in obtaining some of these answers. In the present study, mathematical modelling is used to predict the effects of miRNA on the phosphorylation of and signalling by BCR.ABLp, and on the consequent regulation of tumour suppressor proteins. The purpose of this study is to develop and test our hypotheses that: (i) BCR.ABLp self-regulate its translation through regulation of miRNA expression, (ii) the relative abundance ratio of *BCR.ABL* mRNA and various miRNAs affect BCR.ABLp levels, (iii) inhibition of BCR.ABLp auto-phosphorylation can induce miRNA expression, and a synergistic response of TKI treatment with miRNA/siRNA treatment through BCR.ABLp heterogeneity in CML cells, might ensue.

Methods

Cell culture

Human CML blast crisis cell line K562 (ATCC, Manassas, VA, USA) were used in this study and K562 adherent (K562/Adh) and K562 non-adherent (K562/NonAdh) CML cell suspensions from each T25 cm^2 flask (BD Falcon™, Becton Dickinson, New Jersey, USA) were transferred to individually labelled tubes. The growth medium utilised for culturing of cells consisted of RPMI-1640 (Sigma, Poole UK) supplemented with 10% heat-inactivated fetal bovine serum (FBS; Invitrogen, Paisley, United Kingdom), 2 mM L-glutamine (SAFC Bioscience) and 100 U mL^{-1} penicillin and 100 μg mL^{-1} streptomycin (Sigma-Aldrich, Castle Hill, Australia).

microRNA extraction procedure

The RNA extraction methodology of TRIZOL reagents were used to isolate total RNA including miRNAs. Cell suspensions were harvested for RNA extraction with 1 mL TRIZOL Reagent (Life Technologies Ltd, Paisley, UK) to induce cell lysis. The homogenised samples were incubated for 5 min at room temperature before adding 0.2 mL of chloroform per 1 mL of Trizol (BDH, VWR International Ltd). RNA was precipitated from the aqueous phase by mixing with a mixture of 0.5 mL 100% isopropyl alcohol per 1 mL of TRIZOL (Propan-2-ol, Fisher Scientific). The RNA pellet was air-dried for 5–10 min and the final RNA pellet was re-suspended in 20–25 μL RNase-free water (QIAGEN GmbH, Hilden, Germany). Finally, the RNA was incubated in a block heater (Stuart SBH130DC, Keison) at 60 °C for 10 min. The resultant 30 μL volume of extracted total RNA from each lysates was quantified using the Nanodrop UV spectrophotometry platform (NanoDrop ND-1000-Spectrophotometer, NanoDrop technologies). Extracted miRNA samples were then stored at −8 °C until profiling.

RT-qPCR based miRNA profiling

Samples were sent to Biogazelle, Belgium, for RT-qPCR based miRNA profiling. The method utilised is a validated, high throughput RT-qPCR based miRNA profiling method employing hydrolysis probes and primers from Applied Biosystems as reported by ref. 33. Briefly, expression profiling of 755 miRNAs was analysed with qbasePLUS version 2.0. Quantification cycle (Cq) values were normalised by the geometric mean (global mean) of the relative quantities of all the miRNAs expressed in two samples of K562/Adh and K562/NonAdh cell lines. Global means were calculated by the following steps using qbasePLUS: (1) all Cq values above 32 were considered as noise and excluded from further analysis, (2) conversion of Cq values into relative quantities (RQs), (3) calculation of a sample-specific normalisation factor (NF) as the geometric mean of the RQs of the targets expressed in all samples (common targets), and (4) conversion of RQs into normalised RQs (NRQs) by dividing the RQs by the sample specific NF.[33]

RT-qPCR data from K562 cells

The cell sub-lines utilised in this study were cultured simultaneously and analysed for gene expression by RT-qPCR, following the MIQE guidelines.[34] RT-qPCR amplifications were carried out in 384-well plates using a Roche LightCycler 480 (LC480). Standard curves were set-up using synthetic BCR-ABL template oligonucleotides (sTO) for each assay. Each 10 μL reaction mixture contained 0.1 μL of (20 μM) forward and reverse sequence-specific primers (Metabion International AG, Martinsried, Germany); 0.1 μL of 10 μM fluorescently labelled Locked Nucleic Acid (LNA) probe (Universal Probe Library, Roche, Switzerland), 5 μL of master mix (FastStartTaq DNA polymerase, reaction buffer, dNTP and 3.2 mM $MgCl_2$) and 4 μL of nucleic acid extract. PCR plates were sealed thoroughly with a clear adhesive foil (Roche Diagnostics, Switzerland), briefly vortexed, and centrifuged for 30 s at 4000*g* before being analysed on a LC480 RT-qPCR platform (Roche Diagnostics, Switzerland).

Single cell RT-qPCR

Using fluorescence activated cell sorter (FACS) (BD Influx cell Sorter, BD Biosciences, San Jose, CA, USA) K562 cells from an adherent cell population were sorted directly into 96-well microtitre plates for RT-qPCR. qPCR was performed using a Roche LightCycler 480 (LC480) and the AmpliGrid Single Cell One-Step RT-PCR Kit (Advalytix, Olympus Life Science Research Europa GmbH, Germany) with BCR-ABL primers and probes. Sixty nine cells were selected at random for inclusion in our analyses. Absolute quantification of transcript copy numbers in each single cell was determined from parallel reactions of synthetic template oligonucleotides (sTOs).

Protein phosphorylation analysis in single cells

The Proximity Ligation Assay (PLA) (Duolink *in situ* PLA™; Olink Bioscience, Uppsala, Sweden) was used to detect BCR-ABL specific phosphorylation of Phospho-BCR Y177 as a measure of the BCR phosphorylation status in single cells. Cells were obtained using a similar FACS procedure as described for single cell RT-qPCR. Cells were either analysed for transcripts or for phosphorylated BCR-ABL; it was not possible to perform

both analyses on the same cell. Phospho-BCR (Tyr177) antibody (Cell Signalling Technology, Beverly, MA, USA) was used to detect endogenous levels of BCR and BCR-ABL phosphorylated at tyrosine 177. Primary antibody was diluted (anti-phospho-BCR (Tyr177); 1 : 50 dilution) in permeabilising reagent (Reagent B of Fix & Perm kit) and used to resuspend cells followed by incubation for 60 minutes at room temperature. After incubation, cells were washed twice in PBS/2% FBS, and then resuspended in 0.10 mL secondary antibody solution (anti-rabbit IgG Alexa Fluor 568 conjugate [Cell Signalling Technology, Beverly, MA, USA]; 1 : 50 diluted in PBS) and incubated at room temperature for 60 minutes in the dark. Finally cells were washed in PBS and analysed by CyFlow ML (Partec GmbH, Muenster, Germany) FACS. Secondary antibody alone was used as a negative control. Sixty six cells were selected at random for measurement of the number of BCR.ABLp∼P molecules they contained.

Analysis of the experimental data

The primary data consisted of BCR.ABLp∼P molecules measured in 66 cells and *BCR.ABL* mRNA measured in 69 different cells. Ideally we would have wanted to have both the protein and the mRNA measured in the same cells, but this is not yet feasible experimentally. As perhaps expected our model predicted the number of BCR.ABLp∼P molecules in a cell to increase monotonically with the number of BCR.ABL mRNA molecules in a cell. In our data analysis we therefore used this assumption: we ordered both the protein and the mRNA data set in terms of decreasing numbers of molecules. We then had to deal with the problem that the two data sets were unequal in size (*i.e.* 69 *versus* 66). We drew three random numbers between 0 and 70 (which led to 33, 66 and 67) and we removed the 33rd, 66th and 67th number in the mRNA data set. We then plotted the remaining 66 data points on BCR.ABLp∼P *versus* the 66 data points on *BCR.ABL* mRNA (see the triangles in Fig. 2). The complete data analysis is in the ESI† (Tables S1 to S3).

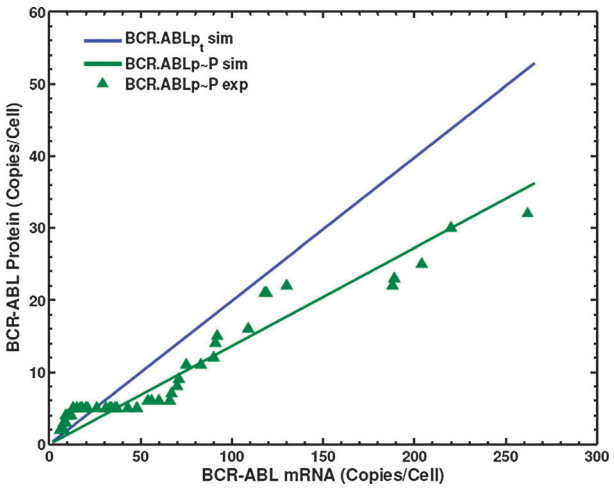

Fig. 2 Correlation of BCR.ABLp∼P protein to *BCR.ABL* mRNA as determined experimentally (triangles) and as calculated by the model (solid green line), the solid blue line shows the model simulated total BCR.ABLp$_t$ protein with the mRNA. The experimental correlation was based on measurements of the mRNA and BCR.ABLp∼P copy numbers in two times 66 individual cells in a single population and the assumption that the BCR.ABLp∼P increased monotonically with the mRNA. The model was based on the mechanism shown in Fig. 1.

Model development

A steady state model was developed to quantify the miRNA repression of mRNA translation. The model is in accordance to Fig. 1 and is a representation of miRNA-mediated repression of *BCR.ABL* mRNA translation to *BCR.ABLp* in CML cells. The miRNAs, miR203, miR451 and miR103 bind with *BCR.ABL* mRNA so as to inhibit the translocation to the ribosome and subsequent *BCR.ABL* mRNA translation. We have modelled equilibrium binding of mRNA and miR by grouping all miRNAs (miR203, miR451 and miR103) together using a conglomerate dissociation equilibrium constant K_{d1}:

$$\mathrm{mRNA} + \mathrm{miR} \Leftrightarrow \mathrm{mRNA}\cdots\mathrm{miR} \quad (1)$$

$$K_{d1} = \frac{[\mathrm{mRNA}][\mathrm{miRNA}]}{[\mathrm{mRNA}\cdots\mathrm{miRNA}]} \quad (2)$$

The value of K_{d1} was calculated to equal 1.5 fM (Table 1) by using the computed standard Gibbs free energy change $(\Delta G'_0)$ of -88.2 kJ mol^{-1} for human 3′ UTR of *ABL1* mRNA binding to miRNA-203 reported by ref. 26. Because this dissociation constant is much lower than the copy number of miRNA and mRNA, the model is insensitive to its precise magnitude.

The translation of *BCR.ABL* mRNA to its protein was modelled as follows;

$$[\mathrm{BCR.ABLp}]_t = q[\mathrm{mRNA}] \quad (3)$$

where q was taken to be constant (see Table 1). [mRNA] represents the concentration of free *BCR.ABL* mRNA. A mechanistic basis for the proportionality between total BCR.ABL protein and free *BCR.ABL* mRNA assumed here, could be that the protein and mRNA are at steady state, with the rate of protein synthesis proportional to mRNA concentration and the rate of protein degradation first order in protein concentration and otherwise constant. The value of q (see Table 1) would depend on the stability and translation efficiency of the protein.

As indicated in Fig. 1, our steady state model should also account for BCR.ABLp auto-trans-phosphorylation through dimerization of BCR.ABLp···ATP complexes. For each monomer we describe the binding of ATP as:

$$\mathrm{BCR.ABLp} + \mathrm{ATP} \Leftrightarrow \mathrm{BCR.ABLp}\cdots\mathrm{ATP} \quad (4)$$

with

$$[\mathrm{BCR.ABLp}\cdots\mathrm{ATP}] = [\mathrm{BCR.ABLp}]\left(\frac{\mathrm{ATP}}{K'_m}\right) = [\mathrm{BCR.ABLp}]\tau \quad (5)$$

which defines τ as the ATP concentration normalized by the K'_m. BCR.ABP protein dimerizes upon the reception of a signal. In this description we shall assume that the signal is always present, independent of the presence of the protein. In principle, the dimerization can lead to a dimer with no, one or two ATP bound, but we shall here neglect the last possibility.

Table 1 Parameters values used in steady state model

Parameters	Values	Source
K_{d1}	0.0015 pM	Calculated[26]
K_{d2}	15 pM	Assuming similarity with Mig1p binding to yeast DNA[37,55]
q	0.25	Adjusted so as to make Fig. 2 fit
[ATP]	2.2 mM	Ref. 56
K_i	100 pM	Fitting cell proliferation data[36]
K_m	1.0 mM	Ref. 57
K_{d3}	1.0 pM	Assumed
K_{m1}	2 pM	Ref. 37
K_{m2}	2 pM	Ref. 37
k_1/k_2	1	Ref. 37
Cellular volume (K562 cell)	2030 μm^3	Ref. 58
Fraction nuclear volume (K562 cell)	0.25	Estimated
$[D]_t$	19.8 pM	Calculation assuming 3 gene copies per cell confined to the nucleus: $= 2 \times 3/(6.02 \times 10^{23} \times 0.25 \times 2030 \times 10^{-15})$
$[Rp]_t$	90 pM	Calculated so as to make modelled miRNA concentrations fit experimentally determined population average miRNA concentrations measured in adherent (high miRNA) and non-adherent
$\frac{[\text{Phosphatase}]}{[\text{BCR.ABL}\sim\text{P}]}$	0.9	Alvira *et al.*[59] wrote that phosphatase goes up with BCRABLp; the constant 0.9 was found here by trying the model

The heterodimers then engage in transphosphorylation of the other monomer in the dimer:

$$\text{BCR.ABLp}_2\cdots\text{ATP} \Rightarrow \text{BCR.ABLp}_2\sim\text{P} + \text{ADP} \quad (6)$$

The rate at which this occurs is given by:

$$v_3 = k_3[\text{BCR.ABLp}_2\cdots\text{ATP}] \quad (7)$$

The phosphatase removes the phosphate again from BCR.ABLp ~ P:

$$\text{BCR.ABLp}_2\sim\text{P} \Rightarrow \text{BCR.ABLp}_2 + \text{phosphate} \quad (8)$$

$$v_4 = k_4[\text{BCR.ABLp}_2\sim\text{P}] \quad (9)$$

The resulting BCR.ABLp ~ P is the active form of B = BCR.ABLp, which here acts as the protein kinase to Rp. Writing K_{d3} for the equilibrium dissociation constant and neglecting cooperativity, the relative concentrations of B···ATP, B_2, B2···ATP and B_2 ~ P relative to the concentration of the monomer, B, are, respectively, τ, $\frac{B}{K_{d3}}$, $\frac{\tau B}{K_{d3}}$, $\frac{k_3\tau B}{k_4K_{d3}}$. At steady state of the above processes, the fraction of BCR.ABLp that is in the kinase form is:

$$\frac{[\text{BCR.ABLp}\sim\text{P}]}{[\text{BCR.ABLp}_t]} = \frac{2\frac{k_3\tau B}{k_4K_{d3}}}{1+\tau+2\frac{B}{K_{d3}}+2\frac{\tau B}{K_{d3}}+2\frac{k_3\tau B}{k_4K_{d3}}}$$

with:

$$[\text{BCR.ABLp}_t] = B\left(1+\tau+2\frac{B}{K_{d3}}+2\frac{\tau B}{K_{d3}}+2\frac{k_3\tau B}{k_4K_{d3}}\right)$$

In our model computations for all but the data points at the lowest mRNA, $B \gg K_{d3}$. Also assuming $k_3 \gg k_4$, we shall approximate the above equation by:

$$\frac{[\text{BCR.ABLp}\sim\text{P}]}{[\text{BCR.ABLp}_t]} = \frac{k_3}{k_3+k_4}\frac{[\text{ATP}]}{[\text{ATP}]+\frac{k_4}{k_3+k_4}K'_m} \quad (10)$$

If the phosphatase activity is relatively small, this reduces to:

$$\frac{[\text{BCR.ABLp}\sim\text{P}]}{[\text{BCR.ABLp}_t]} = \frac{[\text{ATP}]}{[\text{ATP}]+K_m} \quad (11)$$

where K_m is the Michaelis–Menten constant for ATP.

TKIs are competitive inhibitors of BCR.ABLp phosphorylation, *i.e.* competitive with ATP.[35] Accordingly, the inhibition by imatinib (Im) was modelled as follows:

$$\frac{[\text{BCR.ABLp}\sim\text{P}]}{[\text{BCR.ABLp}_t]} = \frac{[\text{ATP}]}{[\text{ATP}]+K_m\left(1+\frac{\text{Im}}{K_i}\right)} \quad (12)$$

Im is the imatinib concentration and K_i is its inhibition constant. The parameter K_i was estimated by fitting the experimental data on cell proliferation at various concentrations of imatinib[36] and its value is reported in Table 1.

The model also accounts for the phosphorylation–dephosphorylation cycle of Rp, which is the transcriptional repressor protein of the miRNA gene. The protein is phosphorylated by BCR.ABLp ~ P in the cytoplasm and subsequently translocated to the nucleus (Fig. 1). The Rp ~ P interacts with the upstream repression sequence (URS) of the miRNA gene. It thereby represses the latter and consequently de-represses the translation of *BCR.ABL* mRNA. The Rp is phosphorylated by a monocyclic cascade mechanism using BCR.ABLp ~ P, which is a tryptophan protein kinase. Phosphorylated Rp is dephosphorylated by a protein phosphatase. This monocyclic cascade phosphorylation was modelled as described by Verma *et al.*[37] following the work of Goldbeter and Koshland.[38,39] We there with assumed that both the kinase and the phosphatase are insensitive to their protein product.[40] In such a cascade, the kinase and phosphatase activity correspond to antagonistic signals, which may be summarized by their effective ratio, *i.e.* the 'input signal I':

$$I = \left(\frac{k_1[\text{BCR.ABLp}\sim\text{P}]}{k_2[\text{phosphatase}]}\right) \quad (13)$$

where k_1 and k_2 are the catalytic rate constants (corresponding to V_{max} conditions) of the kinase and phosphatase respectively. The molecular function of the cascade is the regulation of the fractional phosphorylation (f) of Rp:

$$f = \left(\frac{[\mathrm{Rp{\sim}P}]}{[\mathrm{Rp}]_t}\right) \quad (14)$$

The dependence of f on the input signal and on the total amount of Rp is given by the quadratic equation:

$$\frac{[\mathrm{Rp}]_t}{K_{m1}} = \frac{\frac{f}{1-f} - I\frac{K_{m2}}{K_{m1}}}{f(I-1)} \quad (15)$$

where K_{m1} and K_{m2} are the Michaelis constants of the kinase and phosphatase for Rp and Rp∼P, respectively. We here assume that Rp does not bind to DNA and that the binding of Rp∼P to DNA does not alter its interactions with the kinase and phosphatase, such that:

$$[\mathrm{Rp{\sim}P}] = [\mathrm{Rp{\sim}P}_f] + [\mathrm{D{\cdots}Rp{\sim}P}] \quad (16)$$

Once inside the nucleus the active Rp∼P interacts with the URS of the miRNA gene (D) the transcription of which it thereby inhibits:

$$\mathrm{D} + \mathrm{Rp{\sim}P}_f \Leftrightarrow \mathrm{D{\cdots}Rp{\sim}P} \quad (17)$$

$$K_{d2} = \frac{[\mathrm{D}][\mathrm{Rp{\sim}P}_f]}{[\mathrm{D{\cdots}Rp{\sim}P}]} \quad (18)$$

It represses its transcription. The fraction of URS that is devoid of Rp∼P is called f_1:

$$f_1 = \frac{[\mathrm{D}]}{[\mathrm{D}]_t} \quad (19)$$

We assume the degradation of miRNA to be first order in miRNA concentration and the synthesis rate of miRNA to be first order in the concentration of URS that is devoid of Rp∼P, with rate constants k_{miRNAd} and k_{miRNAs} respectively. At its transcription steady state the total miRNA concentration then becomes:

$$[\mathrm{miRNA}]_t = \frac{k_{miRNAs} f_1 [\mathrm{D}]_t}{k_{miRNAd}} = f_1 [\mathrm{miRNA}]_{t,max} \quad (20)$$

where the maximum concentration of miRNA is defined by all the URS being devoid of Rp∼P.

The dissociation equilibrium constant for the miRNA···mRNA complex is much lower ($\ll$1 pM Table 1) than the concentrations of either species (>1 pM), *i.e.* this is a case of tight binding, Consequently, if the maximum miRNA concentration were to exceed the mRNA concentration, the BCR.ABL protein concentration would drop to zero because its synthesis rate would. And if the maximum miRNA concentration were to be substantially smaller than the mRNA concentration, then BCR.ABL expression would always be substantial: for the Rp to be able to regulate BCR.ABL protein expression substantially, the maximum miRNA concentration should be close to the mRNA concentration. Since we here wanted to study the potential for regulation of BCR.ABL by Rp and miRNA, we assumed that the maximal miRNA concentration was always equal to the total *BCR.ABL* mRNA concentration. This implied that we assumed that the noise in mRNA causing the dispersion in mRNA values, correlated strictly with the noise in total miRNA. A mechanism for this could be noise in the regulation of transcription in general. This assumption and possible relaxation thereof need to be studied in the future. The consequence of the assumption is:

$$[\mathrm{miRNA}]_t = f_1[\mathrm{mRNA}]_t \quad (21)$$

All protein–protein and protein–DNA interactions were assumed to be at equilibrium.[41] The nuclear translocation of Rp∼P was considered to be 100% by assuming that phosphorylation is both necessary and sufficient for immediate net nuclear import. Molar balances were applied to all total component concentrations *BCR.ABL mRNA*, *BCR.ABLp*, *miRNA*, Rp and the operator site concentrations of miRNA encoding genes ($[\mathrm{D}]_t$):

$$[\mathrm{mRNA}]_t = [\mathrm{mRNA}] + [\mathrm{mRNA{\cdots}miRNA}] \quad (22)$$

$$[\mathrm{BCR.ABLp}]_t = [\mathrm{BCR.ABLp}] + [\mathrm{BCR.ABLp{\sim}P}] \quad (23)$$

$$[\mathrm{D}]_t = [\mathrm{D}] + [\mathrm{D{\cdots}Rp{\sim}P}] \quad (24)$$

$$[\mathrm{Rp}]_t = [\mathrm{Rp}] + [\mathrm{Rp{\sim}P}_f] + [\mathrm{D{\cdots}Rp{\sim}P}] \quad (25)$$

$$[\mathrm{miRNA}]_t = [\mathrm{miRNA}] + [\mathrm{mRNA{\cdots}miRNA}] \quad (26)$$

Eqn (27) was used when external miRNA was used as a drug in combination with imatinib.

$$[\mathrm{miRNA}]_t = f_1[\mathrm{mRNA}]_t + [\mathrm{miRNA}]_{drug\_dose} \quad (27)$$

Except for the DNA, all concentrations were expressed in terms of the same (whole cell) volume. The computations for the lines in Fig. 2–5 were carried out by taking the value of total *BCR.ABL* mRNA corresponding to any point on the abscissa, inserting this into the above equations and by then solving

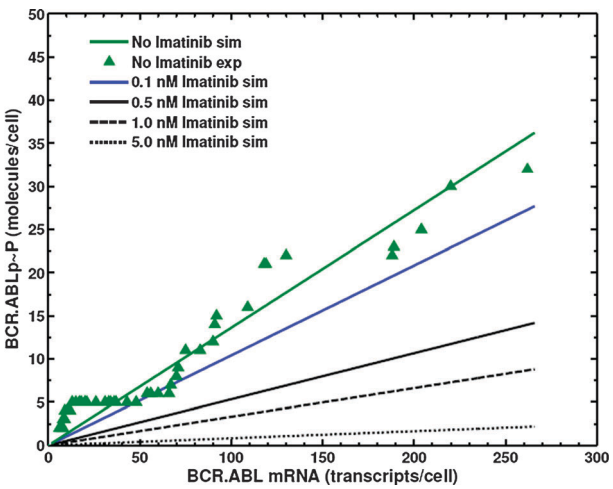

Fig. 3 Model simulated responses of BCR.ABL phosphorylated protein (BCR.ABLp∼P) molecules/copies per cell at various doses (0–5 nM) of imatinib, which inhibits phosphorylation of BCR.ABLp. Imatinib inhibition of BCR.ABLp phosphorylation was taken to be competitive with ATP, as described in the model development. The triangles represent *in vivo* copies of BCR.ABLp∼P as determined experimentally in single cells in the absence of imatinib (see Fig. 2).

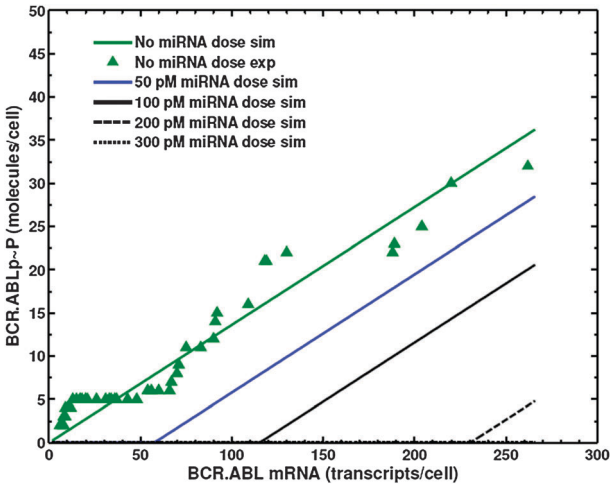

Fig. 4 Model simulated responses of BCR.ABLp∼P molecules/copies per cell at various doses (0–300 pM) of miRNA employed as a therapeutic agent, which inhibits translation of *BCR.ABL* mRNA to BCR.ABLp in CML. The triangles represent *in vivo* copies of BCR.ABLp∼P as determined experimentally in single cells in the absence of miRNA (see Fig. 2).

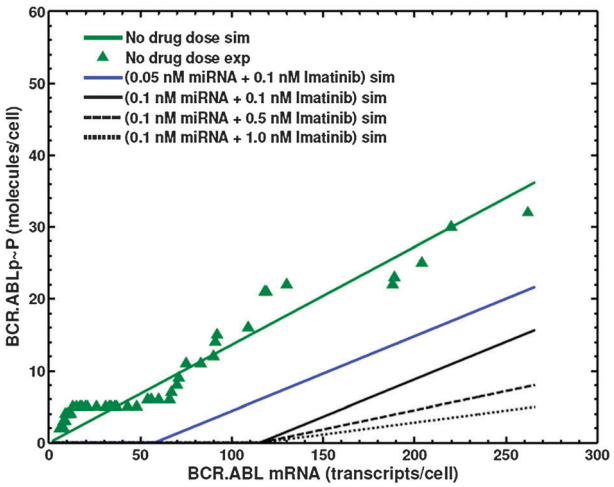

Fig. 5 Model simulated responses of BCR.ABLp∼P molecules/copies per cell at various doses of miRNA (0–0.1 nM) in conjunction with imatinib (0–1.0 nM). miRNA inhibits translation of *BCR.ABL* mRNA to BCR.ABLp and imatinib inhibits phosphorylation of BCR.ABLp respectively, as described in the model development. The triangles represent *in vivo* copies of BCR.ABLp∼P as determined experimentally in single cells in the absence of imatinib.

these equations for total and phosphorylated BCR.ABL protein. The model is computable as follows: I is computed from eqn (13) and the parameters [BCR.ABLp∼P]/[phosphatase] and k_1/k_2; f from I, eqn (15) and parameters K_{m1}, and K_{m2}; [Rp∼P] from f and parameter $[Rp]_t$; [Rp] from [Rp∼P], eqn (25) and (16) and parameter $[Rp]_t$; [D], [D···Rp∼P], [Rp∼P_f] from [Rp∼P], eqn (16), (18), (24) and parameters $[D]_t$ and K_{d2}; f_1 from eqn (19) and parameter $[D]_t$; $[miRNA]_t$ from f_1, eqn (21) and the independent variable $[mRNA]_t$; [mRNA], [miRNA] and [mRNA···miRNA] from $[miRNA]_t$, eqn (2), (22), and (26), and parameter K_{d1}; $[BCR.ABLp]_t$ from [mRNA], eqn (3) and parameter q; [BCRABLp∼P] from $[BCR.ABLp]_t$, eqn (11), and parameters [ATP] and K_m. Parameter values used are given in Table 1. In reality (but see below) the model equations were simultaneously solved using the *fsolve* function in MATLAB 2008Ra (The Math Works Inc., U.S.A.).

Parameter values

Parameter values were estimated on the basis of literature data. We assumed 3 miRNA 'gene' copies per haploid genome and the cells to be diploid for these genes. The total concentration of Rp and the value of q were obtained by fitting to the experimental data on miRNA and BCR.ABPp∼P: in adherent K562cells, in relative units, miR203, miR103a were under non detectable limits and 0.7 miR130b and 0.6 mR451 were found and in non-adherent K562 cells 1.0 miR203, 1.03 miR130a, 1.63 miR130b, and 1.8 miR451. We calculated an average ratio of (0 + 0 + 0.7 + 0.6)/(1 + 1.03 + 1.63 + 1.8) = 0.23, which should correspond to our variable f_1. In our calculations a value of Rp of 90 pM led to a value for f_1 close to 0.2. Using the one but highest-valued data point (because this was positioned close to the straight line fit), we estimated q to amount to 0.25.

Model analysis and simplification

We used the model to calculate the total BCR.ABLp and the BCR.ABLp∼P concentrations as functions of total *BCR.ABL* mRNA and found straight lines through the origin (Fig. 2). We then analyzed the model to examine the background of this phenomenon. We used eqn (13) to calculate I = 10/9 = 1.111, eqn (15) to calculate f = 0.8418, eqn (14) to calculate [Rp∼P] = 75.76 pM, eqn (25) minus eqn (16) to calculate [Rp] = 14.24, eqn (16), (18), (24) to calculate [Rp∼P_f] = 59.92 pM, [D···Rp∼P] = 15.836 and [D] = 3.964, and f_1 = 0.20 from eqn (19). All the above dependent variables are herewith independent of total mRNA concentrations. Because f_1 is constant, eqn (21) makes the total miRNA concentration proportional to the total mRNA concentration. In our model the total miRNA is smaller than the total mRNA. As a consequence, the free mRNA must always exceed the free miRNA, will therefore exceed one tenth of the total mRNA and therefore the very small dissociation constant of the miRNA···mRNA complex. From eqn (2), one then deduces that:

$$\frac{[\mathrm{miRNA}]}{[\mathrm{mRNA}\cdots\mathrm{miRNA}]} = \frac{K_{d1}}{[\mathrm{mRNA}]} \ll 1$$

Consequently:

$$[\mathrm{mRNA}\cdots\mathrm{miRNA}] \approx [\mathrm{miRNA}]_t$$

$$[\mathrm{mRNA}] \approx [\mathrm{mRNA}]_t - [\mathrm{miRNA}] = [\mathrm{mRNA}]_t(1-f_1) - [\mathrm{miRNA}]_{\mathrm{drug\_dose}}$$

Using eqn (3), one then obtains for the total amount of BCR.ABL protein:

$$[\mathrm{BCR.ABLp}\sim\mathrm{P}] \approx [\mathrm{mRNA}]_t q(1-f_1) - q[\mathrm{miRNA}]_{\mathrm{drug\_dose}}$$

And from eqn (12):

$$[\mathrm{BCR.ABLp\sim P}] \approx \left([\mathrm{mRNA}]_t q(1-f_1) - q[\mathrm{miRNA}]_{\mathrm{drug\_dose}}\right) \times \frac{[\mathrm{ATP}]}{[\mathrm{ATP}] + K_m}$$

Inserting the parameter values of Table 1, one obtains in the absence of miRNA drug:

$$[\text{BCR.ABLp}] \approx [\text{mRNA}]_t \times 0.2$$

$$[\text{BCR.ABLp}\sim\text{P}] \approx [\text{mRNA}]_t \times 0.138$$

This reproduces the proportionality produced by the complete model. As an example of the calculation of an individual data point, we take the cell with 220 mRNA molecules, which should then have 30 phosphorylated BCR.ABLp∼P molecules. The inhibition by imatinib may also be calculated for this case, *i.e.* for 0.10 nM imatinib, 23.05 phosphorylated molecules will be left and for 1.0 nM imatinib 7.33. Inhibition by externally added miRNA is calculated by translating this to molecules per cell, assuming equilibration across the plasma membrane. 1 pM corresponds to 0.917 molecule in the cytosolic volume or 1.2 molecules per whole cell (from Table 1), hence 50 pM miRNA correspond to ∼45.85 molecules in the cytosolic volume and ∼60 molecules of miRNA in the whole cell volume. At 220 mRNA molecules in total, and an f_1 of 0.2, there will be 44 miRNA molecules from the cell itself plus 45.85 from the outside. The external miRNA will reduce the free mRNA from 176 to 130, *i.e.* will reduce the phosphorylated BCR.ABL protein from 30 to 22.34. 100 pM miRNA will reduce the number of phosphorylated BCR.ABL molecules to 14.5. Matlab codes of model have been provided in the ESI† and also are available from the authors on request.

Results

Our model may be used for wider applications, but it was here used in an attempt to relate the heterogeneous mRNA levels of *BCR.ABL* between individual cells in a population of CML cells, to the heterogeneous levels of BCR.ABL protein and the phosphorylated form thereof. We assumed that the heterogeneity was not caused by intrinsic noise, *i.e.* dispersion in any of the parameters inside the dynamic network of Fig. 1, but by extrinsic noise, such as dispersion in RNA polymerase activity between cells, which would lead to proportional variation in mRNA and miRNA levels. To enable the model to exhibit complete silencing of translation, the concentration of miRNA was assumed potentially to equal the total mRNA concentration, but normally to be lower than that by a regulatable fraction f_1 (eqn (21)).

Because the expression level of miRNA is regulated by a mono phosphorylation cascade, with a phosphorylated form of BCR.ABLp as the kinase, we determined experimentally the level of *BCR.ABL* mRNA and BCR.ABLp∼P in 69 and 66 individual K562 CML cells, respectively; *i.e.* 135 cells in total. The levels varied substantially from 6 to 262 mRNA molecules per cell and from 2 to 32 BCR.ABLp∼P molecules per cell (see ESI†). Both distributions appeared to be at least bimodal, with the highest peaks around 40 and 5 molecules per cell respectively, but secondary small peaks around 200 and 25, respectively for *BCR.ABL* mRNA and BCR.ABLp∼P.

The assay methodology does not allow measurement of the mRNA and BCR.ABLp∼P copy numbers in the very same cell. We therefore introduced a method of model-inspired data analysis. Our model predicted the BCR.ABLp∼P copy number to increase monotonically with the *BCR.ABL* mRNA copy number. We therefore sorted the assayed individual cells in the order of decreasing number of molecules per cell. This gave us two lists of 69 and 66 data points for mRNA and phosphorylated protein, respectively. We drew three random numbers between 0 and 70 and eliminated the mRNA data points corresponding to these numbers. We then plotted the BCR.ABLp∼P copy number per individual cell *versus* the mRNA copy number per individual cell, yielding the plot of 66 experimental data points of Fig. 2. The heterogeneities measured experimentally at the single cell level (see method section) in both *BCR.ABL* mRNA and BCR.ABLp∼P protein are reflected by the dispersion in the triangles in Fig. 2, i.*e.* mRNA was not varied by variation of some independent variable during experimentation.

Across the range of mRNA, the variation of BCR.ABLp∼P with *BCR.ABL* mRNA appears to be linearly proportional. At the low expression levels, which are characteristic of most cells, there could be nonlinearities, but this is difficult to assess because of effects of binning.

We then used our model to calculate the variation in total and phosphorylated BCR.ABL protein with *BCR.ABL* mRNA. The results of the computations are shown by the solid blue and green lines, respectively, in Fig. 2. The mechanism causing accumulation of BCR.ABLp in CML cells is unclear. However, increased levels of BCR.ABLp are known to promote cell proliferation and survival (resistance).[42] It was hypothesised that increased levels of BCR.ABLp∼P are involved in the adherence properties of CML cells, which cause resistance to TKI treatment. Therefore, BCR.ABLp levels in single cells were simulated with four different doses (0.1, 0.5, 1 and 5 nM) of imatinib, an inhibitor of the tyrosine kinase. Solid blue, black, dashed and dotted lines in Fig. 3 illustrate this respectively. Virtually complete inhibition was predicted to require a dose somewhat exceeding the 5 nM (simulation results not shown) which is in close agreement with an experimental cell proliferation assay with imatinib.[36]

There is a reciprocal regulatory loop between some miRNAs and BCR.ABLp. Important tumour suppressor miRNAs in the BCR.ABL pathway have been shown to be down-regulated in the CML cell population, consistent with ref. 43. This relationship was included in our model, which makes it hard to predict effects of inhibitors and of different type of inhibitors intuitively. Of particular relevance is the issue whether the effect of a drug is related to the level of BCR.ABLp, expression. Fig. 4 shows the model predictions of four doses (50, 100, 200 and 300 pM) of miRNA employed as a bio-therapeutic agent on the heterogeneous population of CML cells expressing BCR.ABLp∼P. Complete inhibition was predicted to require a dose of ∼230 pM. Comparison of model predictions indicate that 5 nM imatinib and 220 pM miRNA should be almost equally inhibitory with respect to the BCR.ABLp∼P levels in these cells. Fig. 5 shows the inhibitory effect of miRNA in

combination with imatinib on the expression levels of BCR.ABLp∼P in the heterogeneous population of CML cells. Model calculations were made for four different combinations, *i.e.* 0.05 nM miRNA + 0.1 nM imatinib; 0.1 nM miRNA + 0.1 nM imatinib; 0.1 nM miRNA + 0.5 nM imatinib and 0.1 nM miRNA + 1 nM imatinib. The 0.4 nM imatinib and 50 pM miRNA should be almost equally inhibitory with respect to the BCR.ABLp∼P levels in these cells. The model also predicts however, that the miRNA should be a much more definitive inhibitor in the lowly expressing cells than the imatinib. In the highly expressing cells the predicted effects of the two inhibitors were additive.

Discussion

Cancer resembles the mal-functioning of a complex network of inter-relationships between genes, gene products and/or proteins that govern plastic processes.[44,45] This then leads to neoplastic processes, requiring the simultaneous deregulation of a number of pertinent genes that act in a cooperative mode, rather than the deregulation of a single gene, or of a set of independently acting genes. In other words, cancer is a systems biology disease[46] and systems biology methods (*e.g.* ref. 47 and 48) should therefore be applied.[49] The goal of the reported study was the generation of a first version of an applied system-wide, data-driven model that incorporates enzymes, RNA and regulatory proteins that are involved in the BCR.ABL expression pathway and that should help predict outcome and response in CML. Systems biology approaches hold the promise to assist molecular pathology by making available novel analytical tools that strengthen the predictive power of transcription data and that can link those data with information on protein levels. Models based on pre-existing knowledge and employing data obtained in robust and sensitive measurements, should help to identify the implications of such new experimental data. Using such models, sensitive analytical techniques used in this context of a systems biology framework, should offer improved diagnostic and screening tools. The results of this paper may serve as one of the first demonstrations of this novel scientific strategy.

A simulation was produced to determine how according to existing knowledge of the regulatory network (Fig. 1) BCR.ABLp may self-regulate its translation through miRNA expression. The simulation of miRNA regulation by BCR.ABLp through Rp (see Fig. 1) took into account how miRNA serves as a controlling factor. The model described the total BCR.ABLp and its relationship to *BCR.ABL* mRNA abundance. This was here taken to help understand the implications of heterogeneity at the single cell level. Model predictions of the BCR.ABLp∼P fraction from total BCR.ABLp correlated with actual BCR.ABLp∼P measurements.[50] Model predictions were here compared with the experimentally observed variation of *BCR.ABL* mRNA with BCR.ABLp∼P between individual cells. The simulated results are in fair proximity to the experimental data indicating that the model is able to capture the experimental BCR.ABLp response to mRNA heterogeneity. We note however three limitations of this validation, *i.e.* (i) that the monotonous increase of BCR.ABLp∼P with total mRNA shown in the experimental data in Fig. 2 results from an assumption, (ii) that the slope of the model-line is the result of fitting, and (iii) that we assumed that the dispersion of both the BCR.ABLp∼P and *BCR.ABL* mRNA were due to noise external to the network of Fig. 1. Therefore the validation of the model is limited to the observation that the model reproduces the quasi-linearity of the experimental variation. Although much more validation of the model is needed therefore, the model does describe the data set, is based on the proposed network in Fig. 1 and should be a better resource for predictions, than the experimental data set itself.

Yet, we caution that any prediction made by the model should be treated as highly preliminary, and should not yet be used clinically at this stage. The model should be further improved through absolute measurements of miRNA in order to check on the predicted heterogeneity of miRNA levels. Additional measurements associated with the pathway would further improve the model including related signalling and regulatory proteins and metabolites. In our model calculations, the miRNA levels were related to total BCR.ABLp levels, and the inhibition of BCR.ABLp auto-phosphorylation was linked to repression and de-repression of a synergistic response/mechanism involving the miRNAs. This should be tested by additional experiments (*e.g.* ref. 51). It should also be noted that our model rests on somewhat arbitrary parameter guesses for the many instances where the actual parameter values are unknown. More experimental work determining the parameter values (*e.g. in vitro* under *in vivo* like circumstances;[52]) will be beneficial for the predictive power of the model. In addition, a probabilistic approach using distributions for parameter values, may be useful.[53] Then the various assumptions we made should be tested experimentally, where measurement of BCR.ABLp∼P and *BCR.ABL* mRNA in the same individual cells, would be a true asset.

One issue with models is whether they are right. A second issue is whether they can be useful, *e.g.* by supporting intuitive predictions that one cannot otherwise be confident upon because the network is complex, by producing counter-intuitive predictions because the network complexity incapacitates intuition, or by suggesting new therapeutic strategies that can then be tested experimentally (*e.g.* in cell cultures or animals). In this specific case, the model may offer insight into the potential for developing improved treatments for BCR.ABL positive CML patients. Indeed, our simulations suggest that, depending on the level of heterogeneity of the cell population, the imatinib dose could be reduced 5 fold while retaining a beneficial therapeutic effect, provided that the miRNA loop could be ascertained to be active and repress BCR.ABLp even if mRNA is highly expressed (Fig. 5). By inhibiting BCR.ABL phosphorylation, imatinib would increase the expression of the miRNA, which would repress total BCR.ABL expression levels and hence even further reduce the level of phosphorylated BCR.ABL protein.

Also, our model showed that depending on the concentrations at which they can be applied, imatinib and miRNA would have different relative effects on cells highly expressing *BCR.ABL* mRNA as compared to less expressing cells.

Consequently limited doses of miRNA might be expected to select for highly expressing cells, whilst similarly effective doses of imatinib would have less such selective effect, and might therefore cause less drug resistance. At high doses, miRNA would eliminate all cells, and might thereby be least selective, but such doses might compromise healthy cells as well.

To characterize disease response to treatment, the extent of heterogeneity of BCR.ABLp within a population of single CML cells in relation to TKI treatment with miRNA/siRNA was analysed. The analysis of transcription has been pivotal in recent analyses aimed at deciphering the mechanisms underpinning progression towards a diseased state. In this respect, major advancements have been made. However there still exist huge technical and knowledge limitations that hinder robust predictions on the basis of transcriptional data alone. Further validation is necessary with more sensitive experimental approaches that can be systematically and iteratively investigated, and fortified with modeling approaches to predict responses with more certainty. This will help to identify and classify the levels of complexity in the disease state of individual (heterogeneous) CML phenotypes, where complexity is due to the negative feedback of increased levels of BCR.ABLp ~ P on miRNAs and the regulatory loop between them in the CML signalling pathways. Imatinib inhibition itself disturbs the regulatory loop, and miRNA-based therapeutics in conjunction with imatinib may further perturb the loop and enhance the treatment of CML. BCR.ABLp tyrosine kinase activity suppresses the expression of miRNAs, and therefore increases BCR.ABLp expression. Disruption of this regulatory loop with miRNAs may improve disproportionately the CML therapy with TKIs by decreasing the abundance of BCR.ABLp.

As shown in Fig. 2, our results predict and show the existence of K562 cells with much higher than average mRNA expression and much higher than average abundance of BCR.ABLp ~ P. Selection of these cells during treatment with less than 1 nM of imatinib would cause resistance of the selected cell population to imatinib if exposed to a dose of 100 pM. In this sense movement from down the *Y* axis of Fig. 3 would represent the disease response to treatment, with the level of phosphorylated BCR.ABLp increasing along the blue line: the cells with the higher mRNA expression levels would be selected for by the therapy. Provided that they could be personalised in terms of the range of mRNA expression observed in the cells of an individual patient, results such as shown in Fig. 3 are also suggestive of a personalised dose for patients. This dose could be tuned to help to avoid side effects, yet to target the cells with the highest actual level of *BCR.ABL* mRNA expression in the particular patient. This would prevent onset of a drug resistance that could manifest if treated with a lower dose of drug.

Conclusion

This study proposed to develop and test hypotheses concerning the regulation of BCR.ABLp through the interplay of miRNAs, *BCR.ABL* mRNA, Rp and BCR.ABLp ~ P. The study has made use of quantitative measurements of *BCR.ABL* mRNA and BCR.ABL protein in single cells, and these have been applied to a new mathematical model of the BCR.ABL regulation. The study commenced with a relatively simplistic model that only takes into account the key components of BCR.ABL biosynthesis. Despite the basic nature of the model, predictions matched actual measurements, although the validation power of this was limited. A future kinetic model should incorporate other modulators affecting the regulation of BCR.ABLp. The present model is amenable to progressive extension to include BCR.ABLp signal transduction and gene regulation including those involving STAT, Ras, GAB2 and Bad2 pathways and may then help understand further factors contributing to cell growth and survival. It is also amenable to personalization by inserting regulatory elements in the network on the basis of individual characteristics implied by individual genome sequencing and deep sequencing of the tumor.[54]

Abbreviations

BCR.ABL	Gene associated with many cases of CML
CBL	Casitas B-lineage factor
CML	Chronic myeloid leukaemia
Cq	Quantification cycle
CRKL	Crk-like factor
FAK	Focal Adhesion Kinase
Grb	Growth factor receptor-bound factor
K_d	Dissociation equilibrium constant
miRNA	microRNA
miR	microRNA
PI3-K	PI3kinases
Rp	Repressor protein
siRNA	Small interfering RNA
TKI	Tyrosine kinase inhibitor
Xp	Protein encoded by gene X

Competing interests

The authors declare that they have no conflicting interests.

Authors' contributions

EK, RB and PD are responsible for the primary experimental data, MV, EK and PD for defining the network to be modelled, MV for the modelling, HW for improving it and producing the simplified analytic version, SR and HW for the systems biology aspects, MV and HW for the processing of the primary data, and HW and PD for the consistency and completeness of the manuscript.

Acknowledgements

Hans V. Westerhoff, Malkhey Verma and Samrina Rehman thank the transnational Systems Biology of MicroOrganisms (SysMO) and ERASysBioprogram and its funders EPSRC/BBSRC for supporting the following projects (R111828, MOSES project,

ERASysBio, BB/F003528/1, BB/C008219/1, BB/F003544/1, BB/I004696/1, BB/I00470X/1, BB/I017186/1, EP/D508053/1, BB/I017186/1). Hans V. Westerhoff also thanks other contributing funding sources including the NWO, and EU-FP7 (EC-MOAN, UNICELLSYS).

References

1 S. Fader, M. Talpaz, Z. Estrov and H. M. Kantarjian, *Ann. Intern. Med.*, 1999, **131**, 207–219.
2 J. Groffen, J. R. Stephenson, N. Heisterkamp, A. de Klein, C. R. Bartram and G. Grosveld, *Cell*, 1984, **36**, 93–99.
3 M. W. N. Deininger, S. Vieira and R. Mendiola, *Cancer Res.*, 2000, **60**, 2049–2055.
4 P. Vigneri and J. Y. J. Wang, *Nat. Med.*, 2001, **7**, 228–234.
5 S. Salesse and C. M. Verfaillie, *Oncogene*, 2002, **21**, 8605–8611.
6 J. R. McWhirter and J. Y. Wang, *EMBO J.*, 1993, **12**, 1533–1546.
7 A. Gotoh, K. Miyazawa, K. Ohyashiki, T. Tauchi, H. S. Boswell, H. E. Broxmeyer and K. Toyama, *Exp. Hematol.*, 1995, **23**, 1153–1159.
8 Y. Le, L. Xu, J. Lu, J. Fang, V. Nardi, L. Chai and L. E. Silberstein, *Am. J. Hematol.*, 2009, **84**, 273–278.
9 J. S. Damiano, L. A. Hazlehurst and W. S. Dalton, *Leukemia*, 2001, **15**, 1232–1239.
10 I. R. Radford, *Curr. Opin. Invest. Drugs*, 2002, **3**, 492–499.
11 A. Hochhaus, S. Kreil, A. S. Corbin, P. L. Rosée, M. C. Müller, T. Lahaye, B. Hanfstein, C. Schoch, N. C. P. Cross, U. Berger, H. Gschaidmeier, B. J. Druker and R. Hehlmann, *Leukemia*, 2002, **16**, 2190–2196.
12 C. B. Gambacorti-Passerini, R. H. Gunby, R. Piazza, A. Galietta, R. Rostagno and L. Scapozza, *Lancet Oncol.*, 2003, **4**, 75–85.
13 J. F. Apperley, *Lancet Oncol.*, 2007, **8**, 1018–1029.
14 T. O'Hare, D. K. Walters, E. P. Stoffregen, T. Jia, P. W. Manley, J. Mestan, S. W. Cowan-Jacob, F. Y. Lee, M. C. Heinrich, M. W. N. Deininger and B. J. Druker, *Cancer Res.*, 2005, **65**, 4500–4505.
15 J. Faber, R. I. Gregory and S. A. Armstrong, *Cancer Cell*, 2008, **13**, 467–469.
16 V. Ambros, *Nature*, 2004, **431**, 350–355.
17 Z. Duan, R. E. Person, H.-H. Lee, S. Huang, J. Donadieu, R. Badolato, H. L. Grimes, T. Papayannopoulou and M. S. Horwitz, *Mol. Cell. Biol.*, 2007, **27**, 6889–6902.
18 I. Bentwich, A. Avniel, Y. Karov, R. Aharonov, S. Gilad, O. Barad, A. Barzilai, P. Einat, U. Einav, E. Meiri, E. Sharon, Y. Spector and Z. Bentwich, *Nat. Genet.*, 2005, **37**, 766–770.
19 G. A. Calin, R. Garzon, A. Cimmino, M. Fabbri and C. M. Croce, *Leuk. Res.*, 2006, **30**, 653–655.
20 S. Volinia, G. A. Calin, C.-G. Liu, S. Ambs, A. Cimmino, F. Petrocca, R. Visone, M. Iorio, C. Roldo, M. Ferracin, R. L. Prueitt, N. Yanaihara, G. Lanza, A. Scarpa, A. Vecchione, M. Negrini, C. C. Harris and C. M. Croce, *Proc. Natl. Acad. Sci. U. S. A.*, 2006, **103**, 2257–2261.
21 J. Lu, G. Getz, E. A. Miska, E. Alvarez-Saavedra, J. Lamb, D. Peck, A. Sweet-Cordero, B. L. Ebert, R. H. Mak, A. A. Ferrando, J. R. Downing, T. Jacks, H. R. Horvitz and T. R. Golub, *Nature*, 2005, **435**, 834–838.
22 J. Lu, G. Getz, E. A. Miska, E. Alvarez-Saavedra, J. Lamb, D. Peck, A. Sweet-Cordero, B. L. Ebert, R. H. Mak, A. A. Ferrando, J. R. Downing, T. Jacks, H. R. Horvitz and T. R. Golub, *Nature*, 2005, **435**, 834–838.
23 F. Fazi, S. Racanicchi, G. Zardo, L. M. Starnes, M. Mancini, L. Travaglini, D. Diverio, E. Ammatuna, G. Cimino, F. Lo-Coco, F. Grignani and C. Nervi, *Cancer Cell*, 2007, **12**, 457–466.
24 L. Zhang, J. Huang, N. Yang, J. Greshock, M. S. Megraw, A. Giannakakis, S. Liang, T. L. Naylor, A. Barchetti, M. R. Ward, G. Yao, A. Medina, A. O'Brien-Jenkins, D. Katsaros, A. Hatzigeorgiou, P. A. Gimotty, B. L. Weber and G. Coukos, *Proc. Natl. Acad. Sci. U. S. A.*, 2006, **103**, 9136–9141.
25 J. Takamizawa, H. Konishi, K. Yanagisawa, S. Tomida, H. Osada, H. Endoh, T. Harano, Y. Yatabe, M. Nagino, Y. Nimura, T. Mitsudomi and T. Takahashi, *Cancer Res.*, 2004, **64**, 3753–3756.
26 M. J. Bueno, I. Pérez de Castro, M. Gómez de Cedrón, J. Santos, G. A. Calin, Juan C. Cigudosa, C. M. Croce, J. Fernández-Piqueras and M. Malumbres, *Cancer Cell*, 2008, **13**, 496–506.
27 T. Lopotová, M. Žáčková, H. Klamová and J. Moravcová, *Leuk. Res.*, 2011, **35**, 974–977.
28 N. Iraci, E. Valli and S. Gherardi, *Blood*, 2009, **114**, 351.
29 N. Felli, L. Fontana, E. Pelosi, R. Botta, D. Bonci, F. Facchiano, F. Liuzzi, V. Lulli, O. Morsilli, S. Santoro, M. Valtieri, G. A. Calin, C.-G. Liu, A. Sorrentino, C. M. Croce and C. Peschle, *Proc. Natl. Acad. Sci. U. S. A.*, 2005, **102**, 18081–18086.
30 E. Pelosi, C. Labbaye and U. Testa, *Leuk. Res.*, 2009, **33**, 1584–1593.
31 T. Yoshihara, A. Taguchi, T. Matsuyama, Y. Shimizu, A. Kikuchi-Taura, T. Soma, D. M. Stern, H. Yoshikawa, Y. Kasahara, H. Moriwaki, K. Nagatsuka and H. Naritomi, *J. Cereb. Blood Flow Metab.*, 2008, **28**, 1086–1089.
32 M. Scherr, K. Battmer, T. Winkler, O. Heidenreich, A. Ganser and M. Eder, *Blood*, 2003, **101**, 1566–1569.
33 P. Mestdagh, T. Feys, N. Bernard, S. Guenther, C. Chen, F. Speleman and J. Vandesompele, *Nucleic Acids Res.*, 2008, **36**, e143.
34 S. A. Bustin, V. Benes, J. A. Garson, J. Hellemans, J. Huggett, M. Kubista, R. Mueller, T. Nolan, M. W. Pfaffl, G. L. Shipley, J. Vandesompele and C. T. Wittwer, *Clin. Chem.*, 2009, **55**, 611–622.
35 T. Schindler, W. Bornmann, P. Pellicena, W. T. Miller, B. Clarkson and J. Kuriyan, *Science*, 2000, **289**, 1938–1942.
36 E. G. Karimiani, *PhD thesis*, The University of Manchester, UK, 2012.
37 M. Verma, P. J. Bhat and K. V. Venkatesh, *Biochem. J.*, 2005, **388**, 843–849.
38 A. Goldbeter and J. D. E. Koshland, Jr., *Proc. Natl. Acad. Sci. U. S. A.*, 1981, **78**, 6840–6844.
39 A. Goldbeter and D. E. Koshland, *J. Biol. Chem.*, 1984, **259**, 14441–14447.

40 F. Ortega, L. Acerenza, H. V. Westerhoff, F. Mas and M. Cascante, *Proc. Natl. Acad. Sci. U. S. A.*, 2002, **99**, 1170–1175.
41 M. Verma, P. J. Bhat and K. V. Venkatesh, *J. Biol. Chem.*, 2003, **278**, 48764–48769.
42 M. Copland, A. Hamilton, L. J. Elrick, J. W. Baird, E. K. Allan, N. Jordanides, M. Barow, J. C. Mountford and T. L. Holyoake, *Blood*, 2006, **107**, 4532–4539.
43 S. Suresh, L. McCallum, W. Lu, N. Lazar, B. Perbal and A. Irvine, *J. Cell Commun. Signal.*, 2011, **5**, 183–191.
44 J. J. Hornberg, F. J. Bruggeman, B. Binder, C. R. Geest, A. J. M. B. de Vaate, J. Lankelma, R. Heinrich and H. V. Westerhoff, *FEBS J.*, 2005, **272**, 244–258.
45 J. J. Hornberg, F. J. Bruggeman, H. V. Westerhoff and J. Lankelma, *Biosystems*, 2006, **83**, 81–90.
46 B. Weigelt and J. S. Reis-Filho, *Nat. Rev. Clin. Oncol.*, 2009, **6**, 718–730.
47 F. J. Bruggeman, H. V. Westerhoff, J. B. Hoek and B. N. Kholodenko, *J. Theor. Biol.*, 2002, **218**, 507–520.
48 S. Rossell, C. C. van der Weijden, A. Lindenbergh, A. van Tuijl, C. Francke, B. M. Bakker and H. V. Westerhoff, *Proc. Natl. Acad. Sci. U. S. A.*, 2006, **103**, 2166–2171.
49 S. Rehman, R. Goodacre, P. J. Day, A. Bayat and H. V. Westerhoff, *Arthritis Res. Ther.*, 2011, **13**, 238.
50 C. Miething, C. Mugler, R. Grundler, J. Hoepfl, R. Y. Bai, C. Peschel and J. Duyster, *Leukemia*, 2003, **17**, 1695–1699.
51 S. Rehman, Y. Xu, W. B. Dunn, P. J. R. Day, H. V. Westerhoff, R. Goodacre and A. Bayat, *Mol. BioSyst.*, 2012, **8**, 2274–2288.
52 K. van Eunen, J. Bouwman, P. Daran-Lapujade, J. Postmus, A. B. Canelas, F. I. C. Mensonides, R. Orij, I. Tuzun, J. van den Brink, G. J. Smits, W. M. van Gulik, S. Brul, J. J. Heijnen, J. H. de Winde, M. J. Teixeira de Mattos, C. Kettner, J. Nielsen, H. V. Westerhoff and B. M. Bakker, *FEBS J.*, 2010, **277**, 749–760.
53 E. Murabito, K. Smallbone, J. Swinton, H. V. Westerhoff and R. Steuer, *J. R. Soc. Interface*, 2011, **8**, 880–895.
54 H. Lehrach, R. Subrak, P. Boyle, M. Pasterk, K. Zatloukal, H. Muller, T. Hubbard, A. Brand, M. Girolami, D. Jameson, F. J. Bruggeman and H. V. Westerhoff, *Proc. Comput. Sci.*, 2011, **7**, 26–29.
55 M. R. Parthun and J. A. Jaehning, *J. Biol. Chem.*, 1990, **256**, 209–213.
56 M. Leist, B. Single, A. F. Castoldi, S. Kühnle and P. Nicotera, *J. Emerg. Med.*, 1997, **185**, 1481–1486.
57 P. Charusanti, X. Hu, L. Chen, D. Neuhauser and J. J. DiStefeno III, *Discrete and Continuous Dynamical Systems*, 2004, **4**, 99–114.
58 E. Ferret, C. Evrard, A. Foucal and P. Gervais, *Biotechnol. Bioeng.*, 2000, **67**, 520–528.
59 D. Alvira, R. Naughton, L. Bhatt, S. Tedesco, W. D. Landry and T. G. Cotter, *J. Biol. Chem.*, 2011, **286**, 32313–32323.

